

Polarized-Photon, Scattered-Atom Coincidence Measurements in  $\text{He}^+$ -He Collisions\*

D. H. Jaecks, F. J. Eriksen, W. de Rijk, and J. Macek

*Behlen Laboratory of Physics, University of Nebraska-Lincoln, Lincoln, Nebraska 68508*

(Received 27 May 1975)

Photon-scattered-atom coincidence measurements with polarization analysis of the photons have been made for 3.0-keV  $\text{He}^+$ -He collisions leading to He ( $3^3P$ ) excitation in a charge-transfer process. The phase difference between the scattering amplitudes for  $m_l=0$  and  $m_l=1$  magnetic sublevel formation is an approximately constant function of scattering angle. We propose a theory which predicts the constancy of this phase difference.

Only recently<sup>1,2</sup> have measurements of magnetic sublevel populations been made in ion-atom collisions where the scattering angle is a well-defined experimental parameter. Such measurements are of immediate interest since they provide the information necessary to decide between rotational or radial coupling interactions within the electron-promotion model.

Current measurements have employed a scattered-particle, polarized-photon coincidence technique; for example de Rijk, Eriksen, and Jaecks<sup>1</sup> have measured the polarization of 3889-Å radiation emitted in 3-keV  $\text{He}^+$ -He charge-exchange collisions, and Vassilev *et al.*<sup>2</sup> have reported similar polarization measurements, but of direct excitation, in 150-eV  $\text{He}^+$ -He collisions. Vassilev *et al.* have concluded on the basis of their data that  $\sigma_1$  is small compared to  $\sigma_0$ , where  $\sigma_1$  and  $\sigma_0$  are the partial cross sections for exciting the  $m_l=1$  and  $m_l=0$  sublevels, respectively.

The purpose of this Letter is threefold: (1) to present data which show, contrary to the results at lower energy, that  $\sigma_1 \approx \sigma_0$  for many scattering angles, (2) to show that the phase difference  $\Delta\varphi$  between the  $m_l=0$  and  $m_l=1$  amplitudes is a nearly constant function of impact parameter (an extremely surprising result), and, finally, (3) to present a theory which predicts the constant dependence of  $\Delta\varphi$  upon impact parameter.

The apparatus used for the measurement is shown in Fig. 1. A  $\text{He}^+$  ion beam is crossed with a thermal beam of He atoms formed by a capillary array. Scattered atoms and ions are separated by a parallel-plate analyzer and the neutrals are detected by an electron multiplier (box-grid type). Perpendicular to the scattering plane, 3889-Å photons are collected and analyzed according to their linear polarization. The signal from the photomultiplier is then counted in delayed coincidence with the signal from the neutral-particle detector.

For a given "polarizer" angle  $\beta$ , the delayed coincidence rate  $I(\beta)$  is interpreted using the results of Macek and Jaecks,<sup>3</sup>

$$I(\beta) = C\{28\sigma_0 + 26\sigma_1 + 15(2\sigma_0\sigma_1)^{1/2} \cos\Delta\varphi \sin 2\beta + (30\sigma_1 - 15\sigma_0) \sin^2\beta\}, \quad (1)$$

where  $C$  is a constant. Equation (1) in general describes an "hourglass"-shaped figure on a polar plot of  $I(\beta)$  versus  $\beta$ .

Measured values of the number of coincidences per number of scattered neutrals are shown in Fig. 2 for six scattering angles. In all of the polar plots in Fig. 2, the  $\text{He}^+$  beam is incident from the left along the  $x$  axis and the scattered neutral particles are detected between  $1.00^\circ$  and  $2.00^\circ$  above the positive  $x$  axis, i.e. in the first quadrant. Additional data at  $1.00^\circ$  were taken for polarizer angles of  $22.5^\circ$  and  $112.5^\circ$ , and these data confirm the shape of the curves. One datum point at a given scattering angle and polarizer angle represents an average of at least two 24-h determinations of the coincidence rate. The error bars in Fig. 2 are estimates of the standard deviation of the random-counting error.<sup>4</sup> An important feature of these curves is their rotation

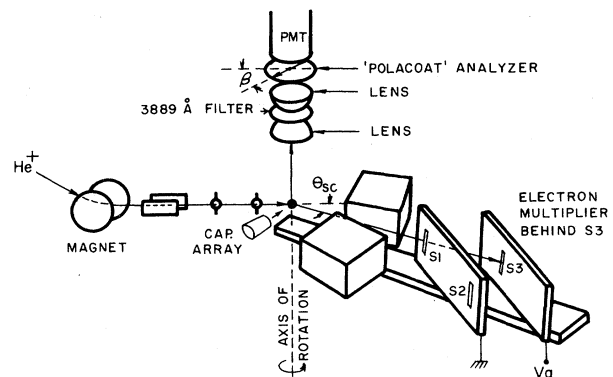


FIG. 1. Schematic diagram of the apparatus.

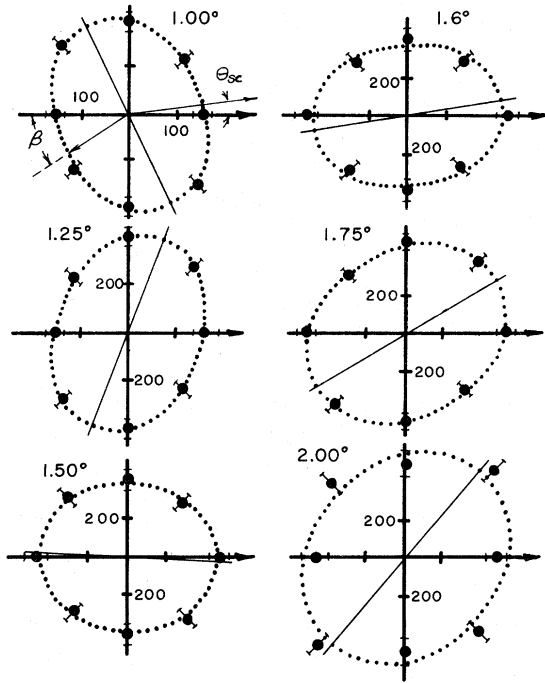


FIG. 2. Plots of  $I(\beta)$  versus "polarizer" angle  $\beta$  for six scattering angles. In all cases the incident beam direction is horizontal to the right and the neutral particle is detected above the positive  $x$  axis. Numbers on the axes represent the scale of the figure in coincidences per  $10^9$  scattered neutrals.

as a function of scattering angle.

The dotted lines in Fig. 2 are computer least-squares best fits of Eq. (1) to the data. From these calculations one can determine  $\Delta\phi$  to within a sign. Figure 3 shows  $\Delta\phi$  versus laboratory scattering angle. One can also determine the quantities  $C\sigma_0$  and  $C\sigma_1$ , the number of measured coincidences per scattered neutral particle for  $m_l=0$  and  $m_l=1$  excitation, respectively. The unknown constant  $C$  is from Eq. (1) and depends, for example, on the efficiencies of the detectors. At a scattering angle of  $1.50^\circ$ ,  $C\sigma_0$  is about  $4 \times 10^{-7}$  coincidences per scattered neutral particle, and there are typically  $2 \times 10^9$  scattered neutrals per hour. For comparison of theory and experiment, more relevant parameters are  $P_0 = C\sigma_0 P_{ex}$  and  $P_1 = C\sigma_1 P_{ex}$ , where  $P_{ex}$  is the charge-exchange probability. The parameters  $P_0$  and  $P_1$  represent the number of measured coincidences per scattered particle, neutral or charged. Using our own measured values of  $P_{ex}$ , we have calculated  $P_0$  and  $P_1$  and they are shown in Fig. 4 versus laboratory scattering angle.

Clearly,  $\Delta\phi$  has the approximately constant

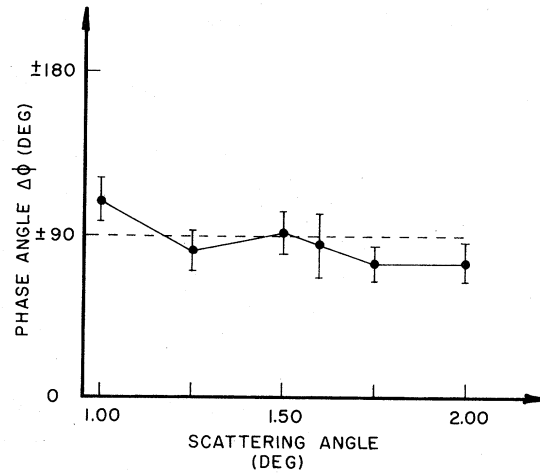


FIG. 3. Phase angle  $\Delta\phi$  versus laboratory scattering angle. Since only linear polarization analysis was made, the sign of the phase is undetermined.

value of  $90^\circ$ . This implies that the rotation of the polarization patterns is due as much to changes in the relative size of  $\sigma_0$  and  $\sigma_1$  as it is to changes in  $\Delta\phi$ . Also, despite the fact that  $\sigma_1$  is small relative to  $\sigma_0$  in the vicinity of  $1.60^\circ$ ,  $\sigma_1$  is nearly equal to  $\sigma_0$  at  $1.00^\circ$ ,  $1.25^\circ$ , and  $2.00^\circ$ . This is to be contrasted to the conclusion of Vassilev *et al.* that  $\sigma_1 \approx 0$ .

We interpret these results using the electron-promotion model, assuming a Landau-Zener transition at a crossing between the  $1s\sigma_g(2p\sigma_u)^2$  and  $(1s\sigma_g)^2 4d\sigma_g$   $\text{He}_2^+$  electronic energy curves at some internuclear distance  $R_0$ . The exact value of  $R_0$  is unimportant for our analysis except to note that it is of the order of 1.0–1.5 a.u.

Because the mean radius of the  $4d$  electron wave function is much larger than  $R_0$ , we suppose that the corresponding molecular energies are degenerate. On the incoming passage of the crossing, the  $4d\sigma_g$  level is populated when the internuclear axis is oriented at an angle  $\sin\alpha = b/R_0$ , where  $b$  is the impact parameter with respect to the incoming beam. Subsequent motion of the nuclei is accompanied only by a phase change of the wave function, since, in the approximation that the  $4d\pi_g$  and  $4d\sigma_g$  levels are degenerate, the charge distribution maintains the orientation it had at the time of the level crossing. A similar transition takes place on the outgoing passage of the crossing. With the assumption that the Landau-Zener transition amplitude  $p$  is small compared to unity due to the two-electron nature of the transition, we have that the wave function

after the collision is

$$\psi \approx p\{\psi_2^{(i)} \exp(i/\hbar) [\int_{-\infty}^{t_i} E_1(t') dt' + \int_{t_i}^{\infty} E_2(t') dt'] + \psi_2^{(o)} \exp(i/\hbar) [\int_{-\infty}^{t_o} E_1(t') dt' + \int_{t_o}^{\infty} E_2(t') dt']\} + \psi_1' \exp(i/\hbar) \int_{-\infty}^{\infty} E_1(t') dt', \quad (2)$$

where subscript 1 denotes the initial  $1s\sigma_g(2p\sigma_u)^2$  level and subscript 2 denotes the  $(1s\sigma_g)^2 4d\sigma_g$  level. The superscripts  $i$  and  $o$  indicate that  $4d\sigma_g$  is evaluated with the symmetry axis along the internuclear axis at the in ( $i$ ) or out ( $o$ ) orientation.

A transformation of the  $4d\sigma$  functions to a frame with the  $z$  axis along the final-beam direction, taking into account that  $4d\sigma_g$  and  $4d\pi_g$  correlate with the  $3p(m_i=0)$  and  $3p(m_i=1)$  atomic orbitals respectively, gives the amplitude  $a_0$  or  $a_1$  that the final level is in the  $m_i=0$  or  $m_i=1$  magnetic substate. We find

$$\begin{aligned} a_0 &= p 2^{-1/2} (3 \cos^2 \alpha - 1) \cos \alpha, \\ a_1 &= ip 3^{1/2} \sin \alpha \cos \alpha \sin \alpha, \end{aligned} \quad (3)$$

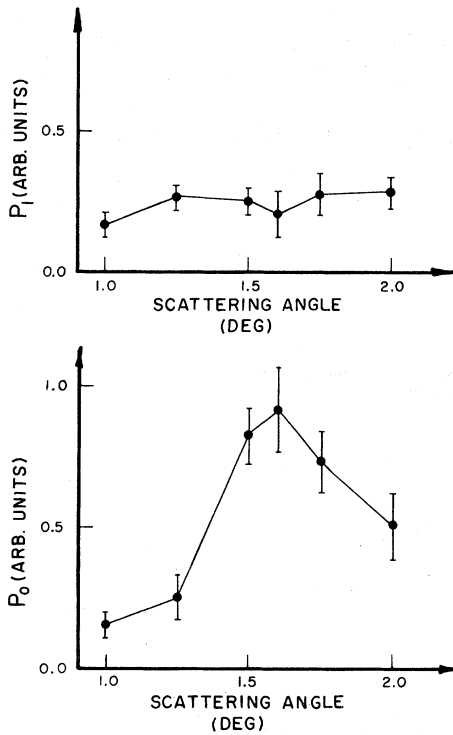


FIG. 4. Probabilities  $P_1$  and  $P_0$  for exciting the  $m_i=1$  and  $m_i=0$  substates as a function of laboratory scattering angle. Here  $P_0$  and  $P_1$  are proportional to the number of coincidences per billion total scattered particles. The number of total scattered particles equals scattered neutrals plus scattered ions.

aside from an overall phase factor. Here  $A = \int_0^{t_o} \{E_2 - E_1\} dt' / \hbar$ .

From Eq. (3) we immediately see that  $\Delta\varphi (=90^\circ)$  is a constant in agreement with the experimental results of Fig. 2. Slight variations around  $90^\circ$  are expected if other mechanisms contribute to the excitation. The model is in excellent accord with the measured phase difference, suggesting that  $3p$  excitation proceeds via the assumed coupling. Note that the phase difference is independent of any assumed relation between impact parameter and scattering angle and any theoretical input concerning the detail of the potential energy curves including the value of  $R_0$ .

In contrast  $|a_0|^2$  and  $|a_1|^2$  are sensitive to all of those parameters. A detailed comparison of this model with the present data has not been made since the requisite potential curves are not available. Furthermore, there is some doubt as to whether a simple relation between scattering angle  $\theta$  and impact parameter  $b$  can be found. If we take  $R_0 \approx 1$  a.u., then since  $a_0(b)$  cuts off sharply at  $b=R_0$ , one expects diffraction maxima and minima<sup>5</sup> separated by  $\Delta\theta \approx \hbar/mvb = 1.57$  mrad  $= 0.09^\circ$ . Since this uncertainty in  $\theta$  is comparable to the angular resolution of the experiment, a detailed calculation incorporating a partial-wave analysis of the scattering is required to fully compare theory and experiment.

\*Work supported by the National Science Foundation.

<sup>1</sup>W. de Rijk, F. J. Eriksen, and D. H. Jaecks, *Bull. Am. Phys. Soc.* **19**, 1230 (1974).

<sup>2</sup>G. Vassilev, G. Rahmat, J. Slevin, and J. Baudon, *Phys. Rev. Lett.* **34**, 447 (1975).

<sup>3</sup>J. Macek and D. H. Jaecks, *Phys. Rev. A* **4**, 2288 (1971).

<sup>4</sup>H. D. Young, *Statistical Treatment of Experimental Data* (McGraw-Hill, New York, 1962), pp. 98 and 111.

<sup>5</sup>R. Shakeshaft and J. Macek, *Phys. Rev. A* **6**, 1876 (1972).